PAPER ID: 1174
DOI: 10.18462/iir.rankine.2020.1174

Energy Recovery From Furnace Off-Gas: Analysis of an Integrated Energy Recovery System by Means of Dynamic Simulation

Daniel ROHDE[(a)], Trond ANDRESEN[(a)], Cristina ZOTICĂ[(b)], Paul WILPERT[(c)]

[(a)] SINTEF Energy Research
Trondheim, 7034, Norway, daniel.rohde@sintef.no, trond.andresen@sintef.no
[(b)] Norwegian University of Science and Technology
Trondheim, 7491, Norway, cristina.f.zotica@ntnu.no
[(c)] Elkem Thamshavn
Orkanger, 7300, Norway, paul.wilpert@elkem.no

ABSTRACT

Surplus heat recovery and electricity generation from furnace off-gas has been implemented at several silicon and ferro-alloy plants in Norway. There is likely significant potential for improvement of both technology elements, system concept, and operation methodology. The main reported issues in current systems include challenging heat recovery due to heat exchanger wear, operation instabilities due to intermittent changes in furnace off-gas conditions, as well as required downtime due to system maintenance.

In this study, an integrated system for energy recovery from furnace off-gas has been analyzed by means of dynamic simulations with Dymola/Modelica. Electricity generation using a steam Rankine cycle and heat export to district heating were included. Efficient operation of the system is challenged by frequently occurring temperature spikes in the off-gas and fluctuating district heating demand. Focus of this study was the comparison of different operation modes to efficiently handle the transient effects and their impact on overall energy system performance.

Keywords: Energy recovery, Electricity generation, Dynamic simulation, System control

1. INTRODUCTION

Elkem Thamshavn is located in Orkanger municipality near Trondheim, Norway. It is an important local employer and a global vendor for advanced silicon products and Microsilica™. The first smelting furnace to produce ferrosilicon commenced operation in 1964. A second larger furnace increased the production in the early 80's. In 1986, Elkem Thamshavn built an advanced energy recovery system, which has continuously been in operation since and made the plant one of the world's leading energy effective silicon producers.

The system recovers energy from the off-gas of two silicon furnaces for electricity generation and heat export. The off-gas shows large fluctuations in temperature and mass flow rate due to collapsing gas bubbles in the furnaces during silicon production. These fluctuations lead to over- and underproduction of steam and material fatigue. To guarantee sufficient margin, only around 80 % of the possible maximum power output of the steam turbine are utilized today. The aim of this study was to analyze how this utilization could be increased. To this end, the energy recovery system was modeled in Modelica and analyzed by means of dynamic simulations. Focus was on different operation modes and their impact on electricity generation.

This paper is structured as follows: The integrated energy recovery system is described in detail in Section 2. The modeling and simulation approach as well as the control structure are explained in Section 3, followed by a presentation and discussion of the results in Section 4. Concluding remarks are given in Section 5.

2. SYSTEM DESCRIPTION

The off-gas from two silicon furnaces is led through a common boiler system, which is producing steam to power a steam turbine and to export heat to the local district heating network. The energy recovery system was built in 1986. An extra evaporator has been added in 2000 by building a steam hood for Furnace 1 and a major

upgrade of the system was performed in 2012, including the installation of several new heat exchanger sections, replacement of the low-pressure turbine rotor, and a new generator. Today, the system produces around 150 GWh per year of electrical energy, which corresponds to roughly 26 % of the electricity demand of the two furnaces. In addition, the local district heating network is supplied with around 15 GWh per year of thermal energy. A schematic of the production process and the energy recovery system at Elkem Thamshavn is shown in Fig. 1.

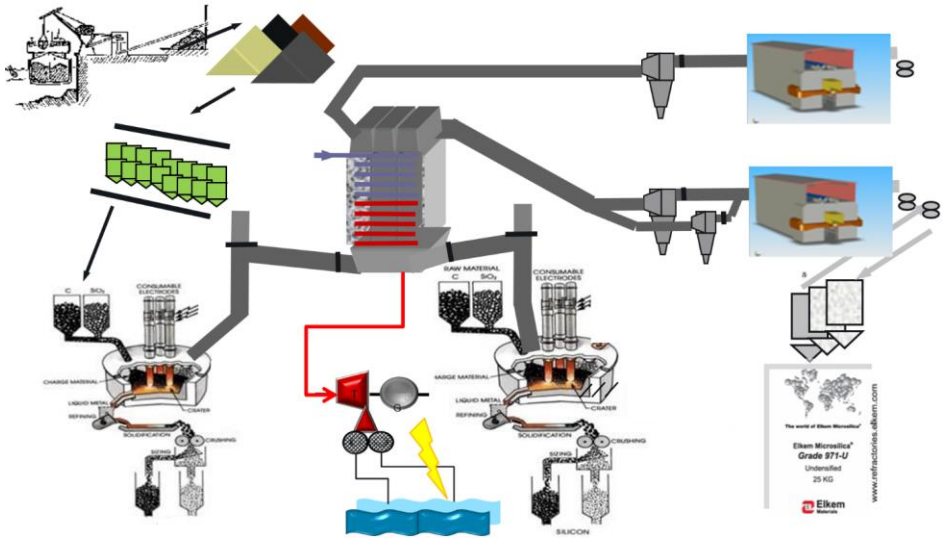

Figure 1: Schematic of production and energy recovery system at Elkem Thamshavn

The system was designed for a pressure of 62 bar but is operated at 55 bar to reduce steam leakages. The produced steam is expanded in a steam turbine, which consists of a high-pressure and a low-pressure turbine. After the high-pressure turbine, steam is extracted to supply heat for the district heating network as well as for feedwater preheating. The steam is condensed in sea-water cooled condensers at a temperature of 36 °C.

Unlike power plants, the system is not optimized for maximum electricity generation. The main aim of the system is to cool the furnace off-gas to ensure stable production. The normal temperature range of the off-gas before the boiler is 700 to 800 °C, but temperature spikes up to 1400 °C can occur. The boiler system thus needs to be operated with good margins for off-gas temperature and steam production. Therefore, the steam turbine runs at around 18 MW on average although it is designed for 22 MW. The goal is to increase the energy output over the next years with focus on furnace process stability, changes in automation, better interaction between steam turbine operation and district heating supply, as well as short-term energy storage. In this study, the changes in automation were investigated. Currently, the off-gas fans are operated manually. However, when the off-gas temperature exceeds 850 °C, an automatic safety function increases the setpoint for the damper positions to increase the air flow rate through the furnaces. The function is deactivated when the off-gas temperature reaches 790 °C. In addition, the emergency stacks are opened when the temperature exceeds 1000 °C. Introducing automatic off-gas fan control could lead to increased electricity generation, lower emissions, and reduced maintenance downtime.

3. DYNAMIC SYSTEM SIMULATIONS

3.1. Methodology

The energy recovery system was modeled using the object-oriented, equation based language Modelica (Modelica Association, 2017) with Dymola Version 2020 as simulation environment. This is an established approach for the analysis of power cycles, see e.g. (Chen et al., 2017) or (Beiron et al., 2019). Component models from the commercially available Modelica library "TIL Suite" (TLK-Thermo GmbH, 2020) and the Modelica Standard Library (Modelica Association, 2020) were used in the system model. Measurement data from the plant were received for a typical winter day and were used as input data for the simulations. A screenshot of the system model is shown in Fig. 2 followed by a description of the main component models and the analyzed operation modes.

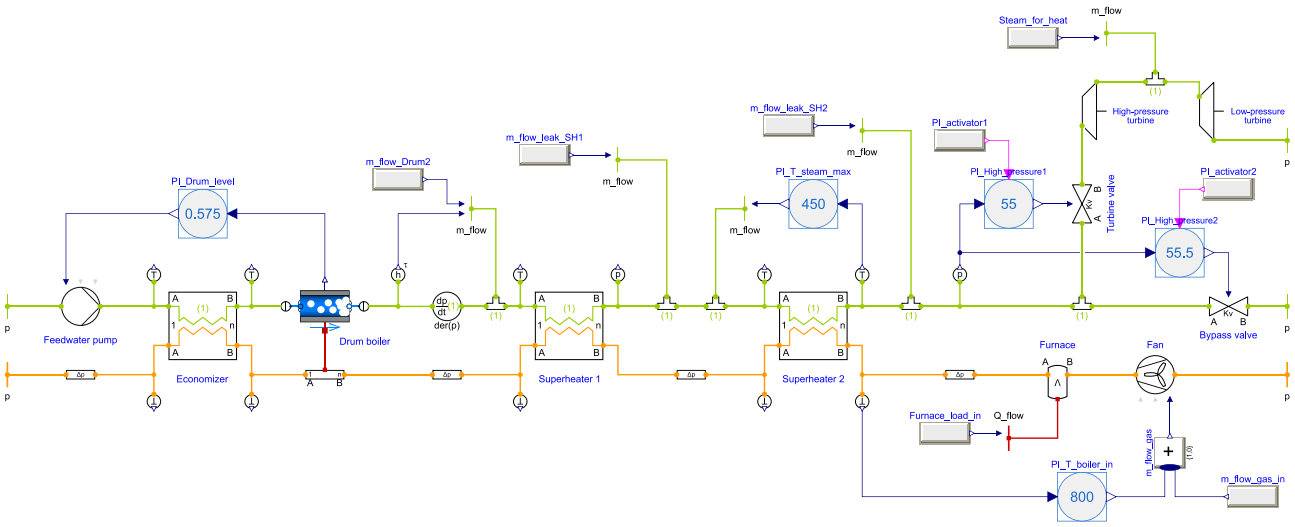

Figure 2: Screenshot of energy recovery system model in Dymola

3.2. Main component models and specifications

Feedwater pump: The feedwater pump model receives the desired mass flow rate as input signal from a PI-controller. It was assumed that the pump can deliver the required pressure lift. The condensers were omitted from the system model and the feedwater inlet temperature was set to 104 °C due to feedwater preheating.

Heat exchangers: The economizer and superheater sections were modeled as counterflow heat exchangers. They were discretized with a finite volume approach and a constant UA-value in each volume. The total UA-values of the economizer and the superheater were set to $1.8 \cdot 10^5$ W/K and $1.5 \cdot 10^4$ W/K, respectively. The superheater was divided into two heat exchanger models because of the attemperator, which can inject water between the superheater sections to avoid unacceptably high turbine inlet temperatures. The pressure drop in the superheater sections was calculated based on a quadratic correlation with the nominal point set to 20 kg/s and 2 bar. Pressure drop in the economizer was neglected.

Drum-boiler: The model "EquilibriumDrumBoiler" from the Modelica Standard Library was included in the system model. It is a simple evaporator model with two states and two-phase equilibrium inside the component is assumed. The model is based on (Åström and Bell, 2000) and is described in (Franke et al., 2003). The heat input was modeled based on a constant UA-value of $1.8 \cdot 10^5$ W/K and the volume of the drum was set to 20 m^3. The steam produced in the steam hood of the Furnace 1 was added to the steam from the drum-boiler.

Furnaces: The furnaces were modeled as a single gas volume, which receives a heat flow rate. This heat flow rate was based on the measurement data and represented the heat input into both furnaces. The volume of the model was set to 400 m^3.

Fans: The three off-gas fans were modeled as one fan, which receives the desired mass flow rate as input signal. This signal was either based on the measurement data or the output of a PI-controller model.

Steam turbine: The steam turbine was modeled with a constant isentropic efficiency of 0.87. Two turbine models were included to represent the high-pressure and the low-pressure part of the turbine. Between the two turbine models, steam is extracted based on the required heat demand for district heating and feedwater preheating. The mass flow rate of the high-pressure turbine is calculated based on Stodola's law of cones (Cooke, 1985). Nominal values were set to 46 bar for the inlet pressure, 14.5 kg/m^3 for the inlet density, 10 bar for the outlet pressure, and 20 kg/s for the steam mass flow rate based on the measurement data. The mass flow rate of the low-pressure turbine was lower compared to the high-pressure turbine due to the steam extraction. The condensation pressure was assumed constant and was set to 0.06 bar.

Control valves: The turbine valve and the bypass valve were modeled with a linear characteristic and maximum Kv-values of 180 m^3/h and 90 m^3/h, respectively. They receive the opening percentage as an input signal.

Leakages: Steam leakages were modeled behind both superheater sections. A quadratic correlation between the pressure and the mass flow rate of leaking steam was assumed. The quadratic function used to calculate the mass flow rate was defined by the nominal points of 1 bar and 0.0 kg/s as well as 57 bar and 0.8 kg/s.

PI-controllers: The PI-controller model from the Modelica Standard Library was extended for increased usability in previous work (Rohde et al., 2018). The model allows numerically stable activation and deactivation of the controller and processes the measurement signal with a first order transfer function to break algebraic loops in the system model. This extended model was used for all PI-controllers in this study. The controllers were tuned by identifying a first order plus time delay model from an open loop step response in the inputs, followed by applying the SIMC tuning rules from (Skogestad, 2003).

3.3. Control structure and operation modes

In this section, the operation of the system is defined in the framework of plantwide control (Zotică et al., 2019). Table 1 shows the manipulated variables (MVs), controlled variables (CVs), and disturbances.

Table 1. Manipulated variables, controlled variables, and disturbances

Manipulated variables	Controlled variables	Disturbances
MV1: Off-gas fan	CV1: District heating supply	D1: Furnace heat load
MV2: Feedwater pump	CV2: Off-gas temperature	D2: Steam from steam hood
MV3: Attemperator	CV3: Drum level	
MV4: Steam turbine valve	CV4: Steam pressure	
MV5: Bypass valve	CV5: Steam temperature	
MV6: Steam extraction		

The control structure of the system is decentralized and formed by PI-controllers with the following MV-CV pairings:

- CV1-MV6: The district heating supply is controlled by the steam extraction.
- CV3-MV2: The drum level is controlled by the feedwater pump.
- CV5-MV3: The steam temperature is controlled by the attemperator.

The remaining three degrees of freedom (MV1, MV4, and MV5) were used to define four different operation modes (cases), which are listed in Table 2 and described below.

Table 2. Case definition

Case name	Fan operation	Steam pressure	MV-CV pairings
Base	Manual	Constant setpoints	MV4-CV4, MV5-CV4
Fan_auto	Automatic	Constant setpoints	MV4-CV4, MV5-CV4, MV1-CV2
Fan_manual_slide	Manual	Sliding	$MV4=MV4^{max}$, $MV5=MV5^{min}$
Fan_auto_slide	Automatic	Sliding	$MV4=MV4^{max}$, $MV5=MV5^{min}$, MV1-CV2

Base: In the base case, the mass flow rate of the off-gas fan (MV1) is based on the measurement data. The steam pressure (CV4) is controlled by the steam turbine valve (MV4) and the bypass valve (MV5) to extend the steady-state operating range for the steam pressure. To minimize throttling losses, MV5 should only be used when MV4 is fully open. This is a two-inputs one-output system for which different control structures can be used, e.g. split range control, valve position control, or two controllers with different setpoints (Reyes-Lúa and Skogestad, 2019). In this study, two controllers with different setpoints were used, which is the operation mode of the plant (55 bar and 55.5 bar, see Fig. 2).

Fan_auto: In this case, the off-gas temperature (CV2) at the boiler inlet is controlled by the off-gas fan (MV1) to increase cycle efficiency and reduce thermal fatigue. The steam pressure is controlled as in the base case.

Fan_manual_slide: In this case, the off-gas fan is operated as in the base case, i.e. based on the measurement data. To minimize throttling losses, the steam turbine valve (MV4) is fully opened and the bypass valve (MV5) is fully closed. This leads to a sliding steam pressure. In practice, minimum and maximum limits for the allowed pressure have to be defined at which the valves would be used again to keep the steam pressure within the allowed range. This was not included in the system model because the pressure always stayed within the allowed limits.

Fan_auto_slide: In this case, automatic fan control is combined with the sliding pressure approach.

All cases were simulated with the simulated time set to 30 hours. During the first 6 hours, the input data are kept constant so that the system was at steady-state at the start of the 24-hour evaluation period.

Measurement data for the disturbances of the process (D1 and D2) as well as for CV1 are shown in Fig. 3 and Fig. 4 below. It can be seen that the furnace heat load ranges from 65 to 90 MW and that it can change relatively fast. The steam mass flow rate from the steam hood also shows high variations and reaches up to 2.5 kg/s. The measured district heating supply for the analyzed day showed slower changes and was around 2 MW.

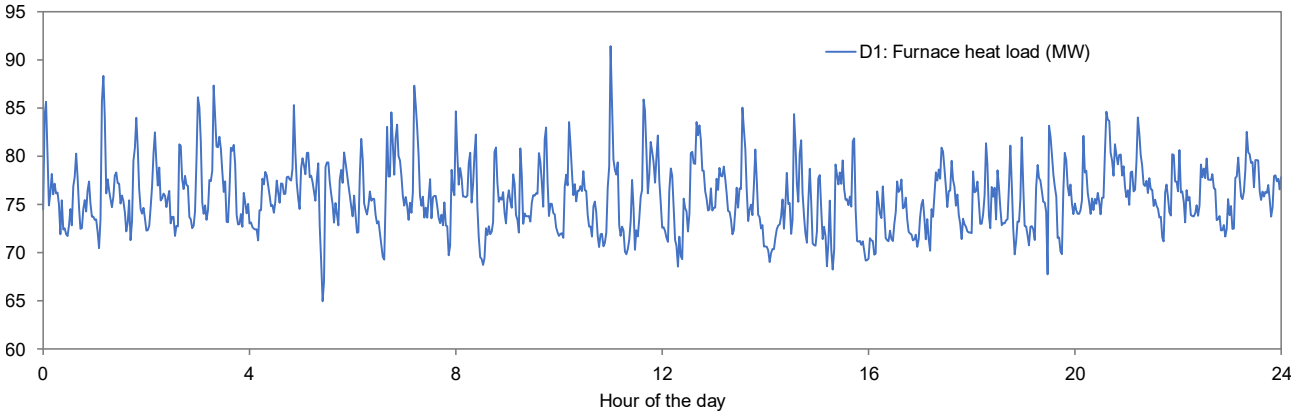

Figure 3: Measured furnace heat load for the analyzed day

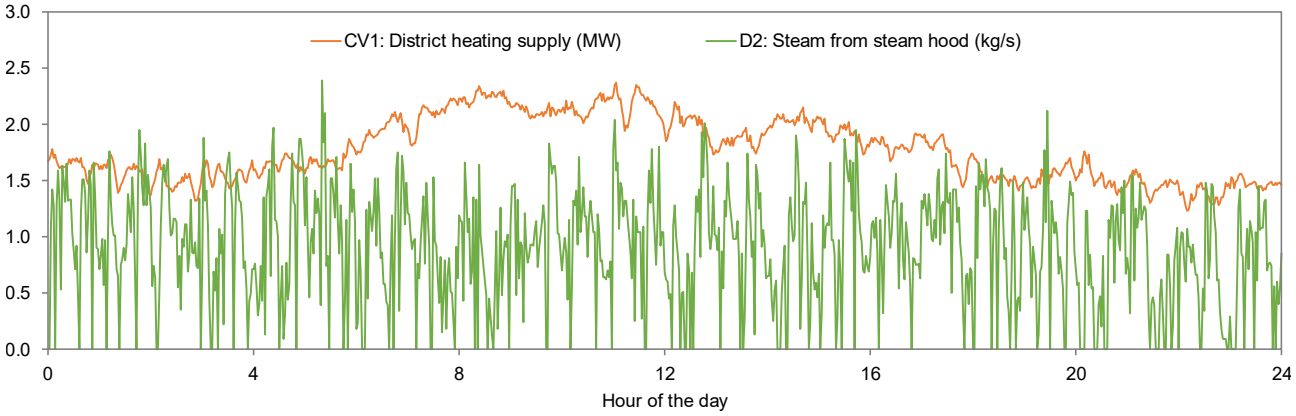

Figure 4: Measured district heating supply and steam from steam hood for the analyzed day

4. RESULTS AND DISCUSSION

In this section, the main results from the simulations are presented and briefly discussed. An important result is the electricity generation during the 24 hours. It is calculated by multiplying the power from the high-pressure turbine and the low-pressure turbine with a generator efficiency of 0.96. The simulated electricity generation for the different cases is shown in Fig. 5.

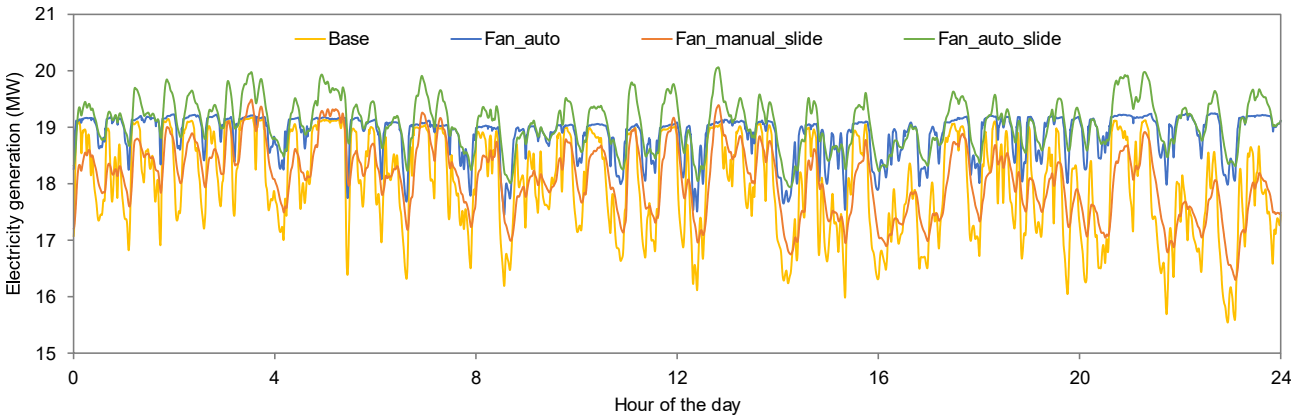

Figure 5: Simulated electricity generation for the four cases

It can be seen from Fig. 5 that the automatic fan control leads to higher and less varying electricity production throughout the day. It stays between 18 and 20 MW while it drops to below 16 MW in the base case. Values for the accumulated electricity generation for the four cases and the measurement data are given in Table 3. The measured value was used to calibrate the component model specifications described in the previous section.

Table 3: Accumulated electricity generation for the four cases during the analyzed day

Case	Measured	Base	Fan_auto	Fan_manual_slide	Fan_auto_slide
Generated Electricity (MWh)	432	432	453	434	458

The simulated electricity generation is around 5 % higher with automatic fan control compared to manual fan control (to recall, manual fan control was used in the Base case). Operation with sliding steam pressure led to an increase compared to fixed pressure operation, but only in the order of 1 %. The steam pressure before the control valves for the four cases is shown in Fig. 6.

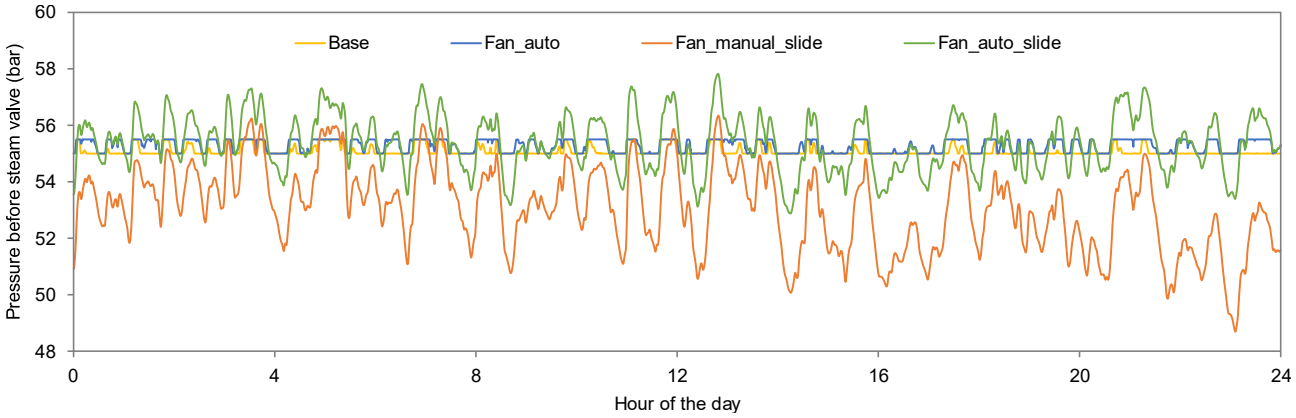

Figure 6: Simulated pressure before the steam valves for the four cases

Fig. 6 shows that the steam pressure varies significantly when sliding pressure is applied. The results show a range from 49 to 58 bar compared to the defined 55 to 55.5 bar for the cases with steam pressure control. Such large variations can increase material fatigue, so the slight increase in electricity generation might not justify this operation mode. Temperature variations are also vital for material lifetime so the off-gas temperature at the boiler inlet is shown in Fig. 7. The effect of pressure control on the inlet temperature was insignificant so only two cases are shown.

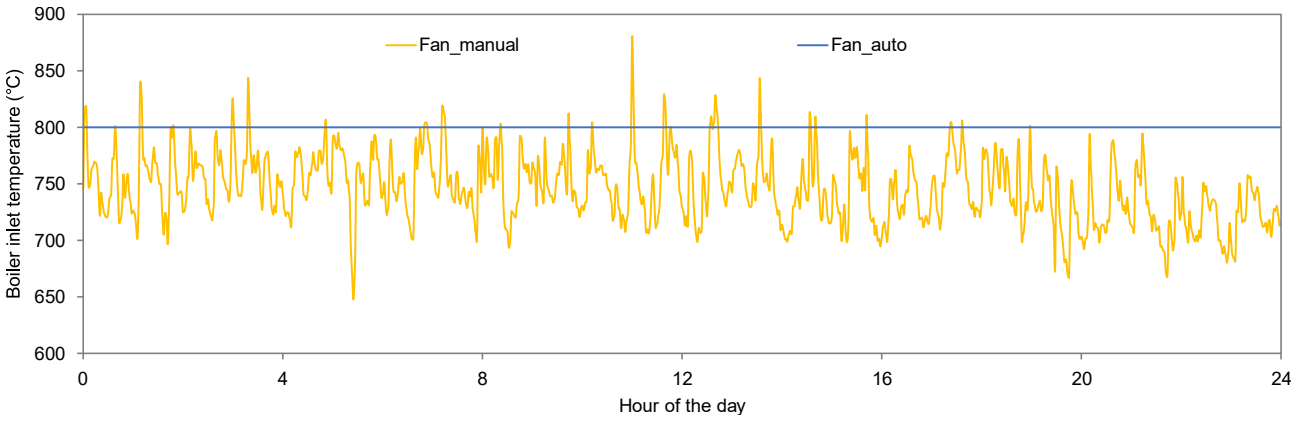

Figure 7: Simulated boiler inlet temperature for manual and automatic fan control

Fig. 7 shows that the boiler inlet temperature varies significantly with manual fan control. These variations lead to thermal stress and increased fatigue of the boiler material. On the contrary, the boiler inlet temperature is kept at the setpoint value with automated fan control. It should be noted though that the automatic fan control probably performs unrealistically well in the simulation model. This is due to the fact that the off-gas ducts were not modeled so there was no delay in the feedback loop.

The off-gas mass flow rate for operation with manual and automatic fan control is shown in Fig. 8.

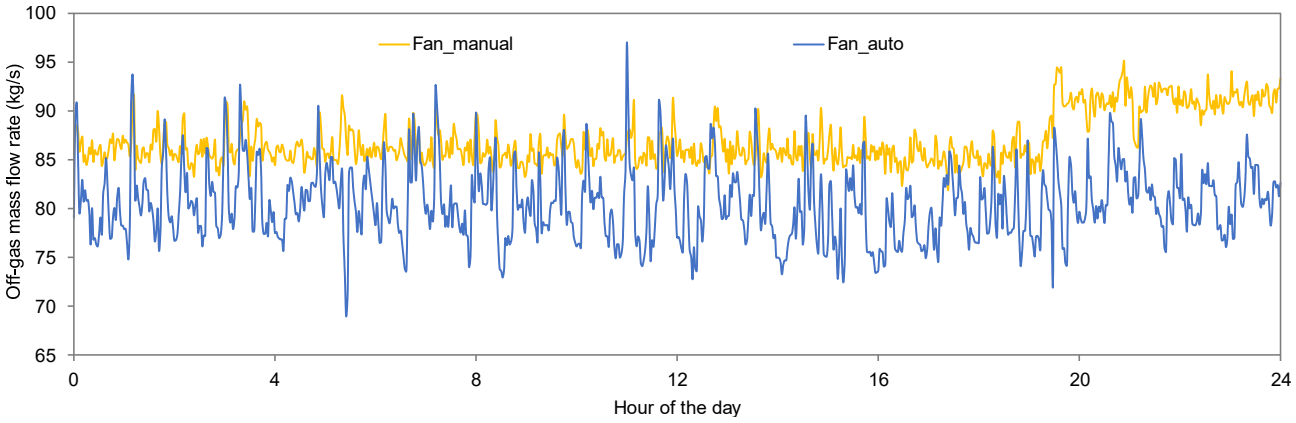

Figure 8: Off-gas mass flow rate for manual (measured) and automatic (simulated) fan control

It can be seen that the off-gas mass flow rate is generally lower with automatic control but shows larger variations. The installed fans run at constant speed and dampers are used to control the mass flow rate. These dampers are sensitive and their position should be changed as little as possible. A more detailed evaluation is needed to decide if the simulated mass flow rate is suitable for the existing system or if it would require the fans with variable speed drives. Such an evaluation was outside the scope of this study.

It should be noted that the results presented above were obtained with measurement data for a single day. Other typical days and/or longer periods should therefore be analyzed to strengthen the results. Also, the measured electricity use of the fans accounted for more than 10 % of the generated electricity for the analyzed day. This electricity use was neglected in this study but should be included in future work to allow the calculation of net generated electricity. Pipes and ducts should also be added to the system model to enable a more realistic analysis of the operation modes. Including a steam storage in the system would allow to avoid bypassing the turbine during fixed pressure operation. This case will be analyzed in future work.

5. CONCLUSIONS

In this study, the operation of an energy recovery system installed at a silicon plant in Norway has been analyzed. A dynamic system model was developed, and four different operation modes were simulated. It was

shown that the automatic fan control clearly outperformed the currently applied manual operation of the fans: An increase in electricity generation of around 5 % was achieved with automatic control. In addition, the inlet temperature to the boiler system was stabilized resulting in reduced thermal fatigue. However, the control of the real system might be more challenging than the control of the simulated system so the results should be seen as an upper bound. In addition, a disadvantage of the automatic fan control is that much larger variations in the damper positions are required, which might lead to reduced damper lifetime. Applying a sliding steam pressure by fully opening the steam turbine valve and fully closing the bypass valve resulted in higher electricity generation compared to keeping the steam pressure at a constant setpoint. However, the increase in electricity generation was minor and might be outweighed by the increased material fatigue due to pressure variation. A more detailed analysis is therefore required before a final recommendation can be made.

ACKNOWLEDGEMENTS

This work was funded by HighEFF - Centre for an Energy Efficient and Competitive Industry for the Future. The authors gratefully acknowledge the financial support from the Research Council of Norway and user partners of HighEFF, an 8-year Research Centre under the FME-scheme (Centre for Environment-friendly Energy Research, 257632/E20).

REFERENCES

Beiron, J., Montañés, R.M., Normann, F. and Johnsson, F., 2019. Dynamic modeling for assessment of steam cycle operation in waste-fired combined heat and power plants. Energy Conversion and Management 198, 111926. doi.org/10.1016/j.enconman.2019.111926.

Chen, C., Zhou, Z. and Bollas, G.M., 2017. Dynamic modeling, simulation and optimization of a subcritical steam power plant. Part I: Plant model and regulatory control. Energy Conversion and Management 145, 324-334. doi.org/10.1016/j.enconman.2017.04.078.

Cooke, D.H., 1985. On Prediction of Off-Design Multistage Turbine Pressures by Stodola's Ellipse. Journal of Engineering for Gas Turbines and Power 107(3), 596-606. doi.org/10.1115/1.3239778.

Franke, R., Rode, M. and Krüger, K., 2003. On-line Optimization of Drum Boiler Startup. 3rd International Modelica Conference, Linköping, Sweden.

Modelica Association, 2017. Modelica® - A Unified Object-Oriented Language for Systems Modeling. Language Specification, Version 3.4.

Modelica Association, 2020. Modelica Libraries. modelica.org/libraries (accessed 20.01.20).

Reyes-Lúa, A. and Skogestad, S., 2019. Systematic Design of Active Constraint Switching Using Classical Advanced Control Structures. Industrial & Engineering Chemistry Research (In Press), doi.org/10.1021/acs.iecr.9b04511.

Rohde, D., Andresen, T. and Nord, N., 2018. Analysis of an integrated heating and cooling system for a building complex with focus on long–term thermal storage. Applied Thermal Engineering 145, 791-803. doi.org/10.1016/j.applthermaleng.2018.09.044.

Skogestad, S., 2003. Simple analytic rules for model reduction and PID controller tuning. Journal of Process Control 13(4), 291-309. doi.org/10.1016/S0959-1524(02)00062-8.

TLK-Thermo GmbH, 2020. TIL Suite – Simulates thermal systems. tlk-thermo.com/index.php/en/software/til-suite (accessed 20.01.20).

Zotică, C., Nord, L.O., Kovács, J. and Skogestad, S., 2019. Optimal Operation and Control of Heat-to-Power Cycles: a New Perspective using a Systematic Plantwide Control Approach. Computer Aided Chemical Engineering 46, 1429-1434. doi.org/10.1016/B978-0-12-818634-3.50239-3.

Åström, K.J. and Bell, R.D., 2000. Drum-boiler dynamics. Automatica 36(3), 363-378. doi.org/10.1016/S0005-1098(99)00171-5.